SOOT DIAGNOSTICS USING LASER-INDUCED INCANDESCENCE IN FLAMES AND EXHAUST FLOWS

R. T. Wainner[*] and J. M. Seitzman[†]

Georgia Institute of Technology
Aerospace Combustion Laboratory
School of Aerospace Engineering
Atlanta, GA 30332-0150

Abstract

Laser-induced incandescence signals are acquired in both a well-documented diffusion flame and a simulated exhaust flow for the purpose of making concentration and particle size measurements. For both types of measurements, the effect on the LII signal of experimental parameters such as gas temperature, particle size, laser fluence, soot composition and morphology are analyzed. Two particle sizing methods are considered, one based on the post-vaporization signal decay rate (conductive cooling rate) and the other by measuring the peak temperatures attained (pyrometry).

The maximum temperatures of different-sized particles are found to be identical ($\pm$ 100 K), removing the pyrometric technique from contention as a particle sizing tool. The signal decay rates are sensitive to particle size, but are, interestingly, insensitive to changes in laser fluence above a certain threshold ($0.1 - 0.5$ J/cm^2, depending on laser wavelength). A numerical simulation of the process overpredicts this signal decay rate, likely due to overestimating the vaporization rate and particle superheat. Varying the laser fluence also did not affect the temperature attained for a given particle size. Likewise, integrated LII signals showed flat or near flat behavior past the fluence threshold. Some evidence of a dependence on beam shape is also observed, in agreement with other research.

Discrepancies were found between the LII measurements of concentration and extinction measurements. Having ruled out other parameters like particle size as the cause of this and noting a significant difference in the signal/volume between the flame and the exhaust flow, the cause is likely due to changing soot composition or structure/agglomeration.

Introduction

Measurement of combustion-generated soot is partly motivated by its role as a pollutant. Respirated soot can cause pulmonary problems and even some types of cancer. Fine particles (less than a few µm) appear to be of primary importance for their ability to penetrate not only into indoor areas but to the depths of the respiratory system.[1] Engine emissions are an important constant source of carbon particulates, and they are naturally highly concentrated in urban areas. The low altitude of these emissions reduces the probability of their being transported away and dispersed by air currents. Particulates such as soot may also cause environmental effects at higher altitudes. They are suspected to be key players in the "greenhouse" warming effect, due to their direct trapping of infrared radiation, and to cloud formation from the increased number of cloud-condensing nuclei.[2]

Soot has engineering implications as well. Soot in combustors can influence local flame temperatures. and also radiation from soot can increase combustor wall or liner temperatures. Thus, the presence of soot can shorten the lifetimes of these parts. Soot is also an indicator of incomplete combustion. Thus, the interest in measuring soot emissions from engines for environmental reasons is accompanied by a desire to understand the processes by which soot is created and destroyed in and around flames. This may help researchers better understand, and thus control, the basic elements of hydrocarbon combustion.

Established techniques exist for measuring soot properties, each with its own limitations. These have included physical sampling,[3,4] laser scattering, and extinction (attenuation).[5-7] A better diagnostic tool for

---

American Institute of Aeronautics and Astronautics

soot measurement, which is accurate, easy, and preferably nonintrusive, is desired. This research focuses on the refinement and analysis of laser-induced incandescence (LII) as a diagnostic tool for soot measurements in flames and exhaust flows. Through modeling and experimental results that address the challenges inherent to LII, we investigate the use of LII for attempting to measure soot concentration and primary particle size. Two size measurement approaches are examined. The first is based on the predicted change in maximum temperature reached by different sized particles. The second exploits the variation in the rate of conductive cooling (after the laser pulse) with particle size.

In this research, we compare results from two environments, a sooty diffusion flame and a simulated exhaust flow. These experiments are intended to determine if parameters such as local chemistry, soot age, or agglomeration may have an effect on soot concentration and particle size measurements. While the simulated exhaust flow represents one of the more common environments for soot measurement, it is also designed to be free of variations in the above parameters. We also compare various properties of the LII signals generated in the two environments, including spectral characteristics and dependence on laser fluence, to determine the similarity of the signals in each, and whether useful comparisons can reasonably be drawn between the two. The experimental results from both environments are also compared to computational models, in order to test the accuracy of the model predictions.

LII Background

Laser-induced incandescence (LII) is a promising tool for soot measurements that combines the best characteristics of some of the more established optical techniques, such as elastic scattering and line-of-sight extinction. Like elastic scattering, LII is an imaging technique with excellent spatial resolution, and it provides a strong signal. Since the signal primarily corresponds to the amount of laser energy absorbed, LII, like extinction, is mostly sensitive to the concentration or volume fraction of soot and only weakly sensitive to particle size. The technique is based on a laser-induced optical signal first observed in the realm of combustion as an interference in Raman measurements in a flame in 1977.[8] Since these early measurements, the physical process behind this signal has been employed and tested for making simple, nonintrusive measurements of combustion-generated solid particulate, or soot.

Laser-induced incandescence of soot occurs when soot particles absorb laser illumination. Soot particles are comprised of branchy aggregates of nominally spherical primary particles of graphitic carbon on the order of a few tens of nanometers in diameter. If the energy absorption rate is sufficiently high, i.e., the laser intensity is high enough (thus pulsed lasers are , typically employed), the particle's temperature will rise to a level where the soot particles will glow (incandesce) noticeably stronger than the background emission (e.g., from non-illuminated particles at the local temperature). This incandescence is a broadband emission, essentially blackbody emission modified by the spectral emissivity of the material.

When the particle reaches a certain temperature (e.g., 3915 K for graphite), vaporization begins to take place at the particle surface. As the temperature of the particle increases, so does the vaporization rate until a balance is attained and the particle temperature levels out. As the laser pulse ends, the temperature drops and the vaporization rate falls with it. During this interval, the dominant cooling mode transitions from vaporization to conductive cooling by the surrounding gas.

The LII signal is nearly proportional to soot concentration because the size of the primary soot particles is in the Rayleigh limit for light absorption, where the particles will absorb (and emit) approximately proportional to their volume or mass. However, the energy loss mechanisms of conduction and evaporation are expected to scale closer to d^2. Thus, it is predicted that primary particle size and gas temperature would affect the volumetric scaling of the LII signal through these cooling mechanisms. Also, since the incandescence is a strong function of temperature, the signal emitted in this last region decays quickly, so is much lower than during the laser pulse. However, shorter delays or sufficiently long gating can produce a measurable signal for delayed detection.

The LII signal becomes less sensitive to energy input beyond the energy required to induce vaporization. This 'threshold' fluence has been determined to be on the order of 0.1 J/cm^2 (10 MW/cm^2) for nanosecond scale, visible or near visible wavelength lasers, and for soot particle sizes typical of those in sooty flames. Therefore, for higher laser fluences, it is thought that average soot temperatures and signals begin to level out as most of the additional energy goes into vaporization.

The actual signal behavior above threshold depends on the the spatial profile of the laser beam or sheet.[9] For typical Gaussian distributions, falling sig-

nals due to vaporization at the center of the beam are countered by increasing signals in the 'wings'. Another consideration is that increasing maximum signals are offset by the sharper signal decays which result from increasing vaporization.[10] Some of the laser energy can go into raising the energy levels of the vaporized molecular carbon species (C_2, C_3). The visible emissions from C_2 can be quite strong for high intensity excitation and are considered an interference as these signals do not scale exactly like LII. The use of infrared excitation or delayed detection has been determined to minimize these contributions.

The model shows that particles of different sizes will reach different maximum temperatures and cool down at different rates. The latter of these effects has been investigated for making measurements of particle size.[11,12] The signal emitted during the post-vaporization period is a function of the size and temperature of the particle just after the vaporization period, the surrounding gas temperature, and the overall conductive cooling rate (see Fig. 1). These particle conditions after the laser pulse are, in turn, a function of the original particle diameter. Smaller particles are expected to cool faster due to their larger surface area to volume ratio. However, the lower particle temperatures at longer times will yield much weaker signals and the cooling should be more sensitive to changes in local gas temperature.
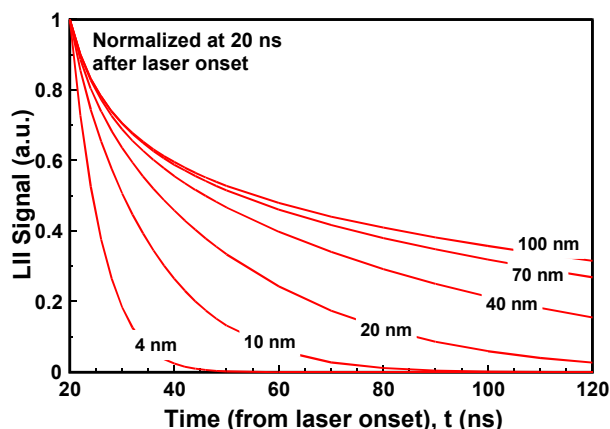
Figure 1. Model results for the signal decay from different sized particles illuminated by a 0.5 J/cm^2 laser pulse at 1064 nm. Detection is at 650 nm. Ambient temperature is 350 K.

Alternatively, Mewes and Seitzman[13] suggested that primary particle size could be monitored by determining the maximum temperatures reached in terms of the relative strength of signals at two different wave-lengths. The higher heating to cooling rate ratio ($\sim d^3/\sim d^2 = \sim d$) of the larger particles should yield higher temperatures. In terms of blackbody radiation, the larger particles would then not only emit more strongly than the smaller particles, but would have their radiation shifted toward the blue (shorter wavelengths). The red/blue ratio monotonically increases as temperature decreases.

Most LII measurements have been performed in small lab flames,[14-18] though other environments have been addressed, including droplet combustion,[17] diesel engine cylinders[20,21] and exhausts.[22] LII signals have generally been calibrated to soot volume fraction measurements from extinction,[15-17,19] or sampling methods.[18] Though results have been reasonably accurate, some discrepancies have been observed.[16,17] Due to the non-volumetric nature of the cooling mechanisms, early model results suggest the response of the LII signal may be dependent on the size of the primary particles. This should be especially true at longer delays where sensitivity to local gas temperature becomes a factor as well. Therefore, an environment with a range of particle sizes and gas temperatures will likely be susceptible to errors in volume fraction measurements. Recent results[23] for nominally spherical particles in an exhaust flow have shown such a particle size dependence to exist.

Experimental Methods

Soot Generator

The combination of a controlled soot field and simulation of an engine exhaust is attained with the use of a soot generator which provides an aerosol of carbon black particles (Fig. 2). The flow at the output of the generator is nonreacting, has no potential interferences associated with the presence of larger hydrocarbons, and is dilute enough to avoid signal trapping. It is also designed to be nearly uniform in temperature, concentration, and particle size.

The aerosol is obtained in the following manner. A dispersion of carbon black (soot) in distilled water (5.6 g C / L H_2O) is prepared with 1 mL gum arabic added per liter of water as an emulsifier. This solution is atomized with the use of an aspirator/impingement type nebulizer (Inspiron), providing a carbon/water fog which is then diluted by a secondary air flow. Phase-Doppler particle analyzer measurements of the nebulizer droplet diameter yielded an average value (D_{10}) of 4 μm, with a 2 μm FWHM for the measured size distri-

3

bution The solution is aspirated with air at a constant flow rate of 9.2 L/min, yielding a solution flow rate of 0.34 mL/min. The carbon black material (Cabot 800) is composed of approximately 17 nm particles.
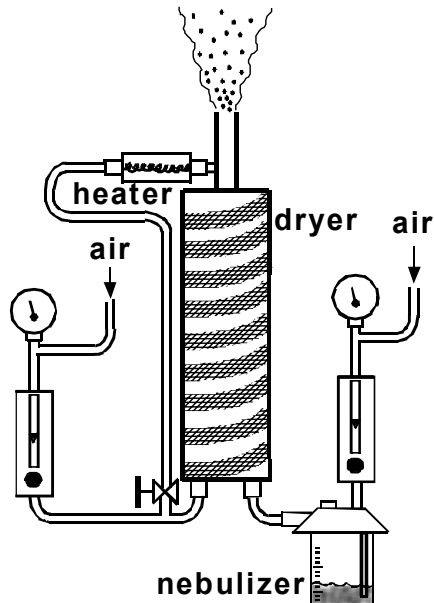
Figure 2. Soot generating experimental apparatus.. Dryer tube is wrapped with heater tape to maintain approximately 100 ºC walls. Separate air flows are monitored with a rotameter and pressure gauge.

Each flow is separately directed into an aluminum drying cylinder (3 in dia., 24 in. long) held vertically. To evaporate the water droplets, the cylinder is heated with heating tape to a nominal temperature of 100 ºC. The resulting suspension of dry carbon particles exits the top of the drying cylinder out a 12 inch long aluminum tube. This soot-laden jet is 15 mm in diameter and measurements are made about 15 mm from the end of the tube.

Small variations (~3×) in the soot aerosol concentration are obtained by changing the secondary air flow rate. Greater dilutions in soot concentration are achieved by further diluting the carbon/water dispersion. This will, however, also change the size of the carbon particles produced. As the carbon laden water droplet evaporates, surface tension and electrostatic forces should cause all the small carbon black particles to form a single, nominally spherical,[24] particle by the time the water is evaporated. Thus the particle size at the generator exit will vary with the cube root of the concentration of the carbon solution. The exit temperature of the jet can also be varied by preheating the secondary air flow, diverting some fraction of it through a

coiled-filament heater (Sylvania - Process Heat). The results presented in this work, however, do not employ this heater with exit temperatures held close to 120 ºC.

Diffusion Flame

The more complex, reacting environment is provided by a well-calibrated, simple, axisymmetric diffusion flame that has been used extensively in a number of soot studies.[4-7,9,10,16,17] The flame is produced by a concentric laminar diffusion flame burner. Ethylene (C_2H_4) was chosen as the fuel for its high sooting tendency. The fuel flows through a central tube of 11.1 mm i.d., surrounded by a concentric flow of air contained in a 101.6 mm i.d. honeycombed outer tube. Matching the data from previous research, the flowrates for fuel and air, respectively, were 3.85 cm^3/s and 713.3 cm^3/s, measured by calibrated rotameters

Laser Excitation

The LII signal is produced by the fundamental (1064 nm) or frequency-doubled (532 nm) output of a Nd:YAG laser (7 ns FWHM) nominally operated at 10 Hz, with maximum pulse energies of 450 mJ and 200 mJ, respectively. When fine spatial resolution is required (e.g., in the flame), the 8 mm (3.5 mm FWHM) diameter beam (measured by a burn mark method and Rayleigh scattering) is focused by a 90 mm diameter, 500 mm focal length fused-silica cylindrical lens to a waist of about 0.2 mm (FWHM). Only the middle ~3 mm or less of the laser sheet is included in the collection volume in order to keep the intensity constant across the imaged region. Laser intensity is varied by employing the combination of a half waveplate and polarizing beam splitter. Most results reported here are for average energy fluences at or greater than 0.1 J/cm^2. The repeatability of pulse-to-pulse laser energy and temporal profile were generally good, with a worse case variation of $\pm$ 7%.

Signal Detection

The LII signal is recorded at a right angle to the laser beam by a photomultiplier tube (Hamamatsu R928B) behind the collection optics of 150 mm and 50 mm spherical lenses, optical filters, and a rectangular aperture (see Fig. 3). This signal is recorded in one of two ways. For spectrally broadband detection, the detector is positioned directly behind this collection system. Finer spectral resolution is achieved by recording signals at the output slit of a half-meter Jarrell

4

Ash monochromator. The two slits are fully open, providing a bandpass of 3.7 nm FWHM and an image width of 0.4 mm. The optical filters include neutral density filters to keep the PMT in its linear operating range, and bandpass filters (650 nm and 430 nm, 10 nm FWHM), Schott colored glass filters, and a 532 nm holographic notch filter for enhancing the rejection of interference from signals at other wavelengths, in particular, elastic scattering.
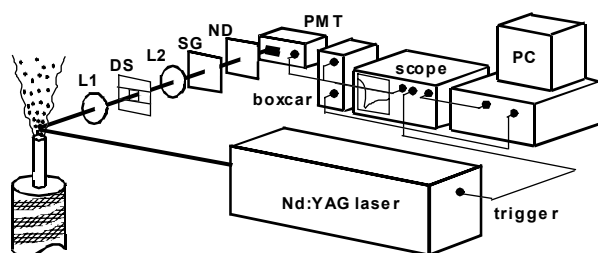
Figure 3. Laser-induced incandescence experimental setup (shown with soot generator). L1: f = 150 mm lens, L2: f = 100 mm lens, DS: height/width-adjustable rectangular aperture, SG: Schott glass filter(s), and ND: neutral density filter(s).

The signals generated at the exit of the soot generator employed broadband detection to increase the sensitivity to the low soot concentrations it yields. 'Red' signals employ simply an RG-630 Schott glass filter before the PMT. Thus the bandwidth is set by the filter (~630 nm) and the 0.1% quantum efficiency point of the PMT (~850 nm). 'Blue' signals are generated with a combination of BG-3 and BG-18 filters (~370 to 450 nm). The image width for these measurements was approximately 7 mm.

Flame data were recorded from the region of maximum soot volume fraction (f_v), and therefore strongest signals, just inside the flamefront. Most of the previously recorded data available for this flame is along this pathline. All the data were acquired using a fixed vertical position for the detector and laser beam, and thus with the same height (intensity) in the laser sheet. Therefore, signals at different heights in the flame were achieved by traversing the flame vertically through the laser sheet. The signals produced by the PMT are recorded (gated, normally for 50 ns, integrated, and averaged) on a digital oscilloscope or a boxcar averager.

Results

Diffusion Flame

Concentration Measurements

Measurements of soot concentration using LII were performed along the path of maximum soot above the burner. Signals were integrated over a 20 ns gate at various delays from the signal onset. Figure 4 compares these signals with extinction data,[17] where all signals have been normalized at the lowest height value. A clear discrepancy with the extinction data is apparent, with a greater deviation for increasing height in the flame. Normalizing the signals at the location of peak concentration (height above burner (HAB) of ~40mm), as is commonly done, masks the difference on a plot such as this. The systematic difference in the measurements is also evident in the lower plot of Fig. 4, which shows the relative error between the LII and the extinction data for the more common calibration at the soot peak signal.
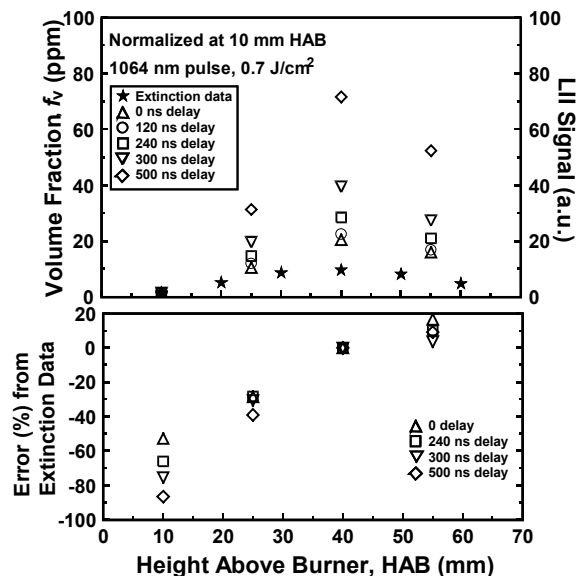
Figure 4. (above) LII signals generated at four heights in the diffusion flame, compared to extinction measurements of soot concentration.[17] Detection is at 430 nm. (below) Relative deviation of the LII signals from the extinction data. Renormalized at 40 nm HAB.

The systematic error in the LII measurements, assuming the extinction data to be accurate, can be explained in part by the predicted increase in signal for larger particles described previously. Briefly, larger particles with their larger volume to size ratio have an increased heating to cooling rate ratio. Thus, the LII

5

signal per unit soot concentration (C) increases for the larger particles. However, the measured variation in C in the flame is about two from the lowest point in the flame to the soot concentration peak, while the model predicts about only a 30% increase in C for the measured primary particle size[23] effect. In addition, C continues to increase above 40 mm HAB, even though measurements[5] show the primary particle size to be relatively constant, with just a slight decrease from 40 to 55 mm HAB. Thus, the monotonic trend of the error plot would suggest that the effect cannot be solely due to primary particle size.

One possibility is the effect of varying local gas temperature in the flame. However, soot zone temperatures have been measured[6] to remain nearly constant from 10 to 50 mm HAB and decrease rapidly after that. Also, the model predicts only a weak sensitivity (~2%) to these sort of gas temperature variations for LII signals observed with detection during and just after the laser pulse, i.e., 'prompt' detection.[*] For detection delayed from the laser pulse by ~100 ns or more, the relative signal variation throughout the flame begins to differ significantly from the results of Fig. 4. This is consistent with the expected increase in dependence on local gas temperature when conductive cooling becomes more important. Thus, it is unlikely that the temperature variation in the flame is the source of the error in the LII concentration measurements. If soot agglomeration, which increases with height in the flame, is a contributor, then the 'effective' particle size may increase monotonically with height in the flame. The systematic LII error may also result from changes in soot composition (aging of the soot).

Primary Particle Size Measurements

Again, two methods were examined for primary particle sizing; post-vaporization signal decay rates and spectral signal ratios for measuring peak temperatures. Results for the LII signal decay rates at different heights in the ethylene flame are shown in Fig. 5. Signals are normalized at 60 ns after the signal onset to

---

[*]This is why prompt detection is ideal for volume fraction measurements. Particle temperatures are expected to be high enough during the laser pulse that variations in the local gas temperature do not have a significant effect on the temperature gradient between the particle and the gas, and hence do not significantly alter the heat conduction rate. Also above the threshold fluence, energy loss through vaporization is expected to dominate conductive cooling.

avoid the influence of short-lived interferences such as C_2 LIF and to isolate the signal behavior during the conduction-dominated period. Observations in this flame are over a limited range of primary particle diameters (14 to 33 nm), but a dependence on particle size (or at least the height in the flame) is apparent for the signal decay.
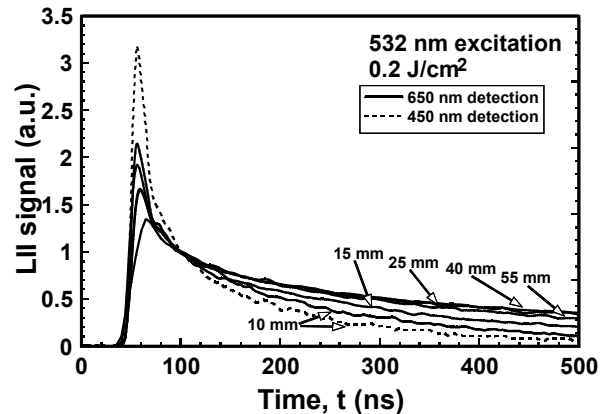
Figure 5. LII signal decay versus time for five heights in the ethylene flame and at two detection wavelengths. Primary particle diameters for these positions are 14, 22, 30, 33, and 31 from lowest to highest height.[5] Laser excitation is a Nd:YAG (532 nm) at 0.2 J/cm². Signals are normalized at 60 ns after signal onset.

First note that the decay rates for detection at 430 nm are larger than for signals detected at 650 nm. This follows from the higher temperature sensitivity of blackbody emission in the blue (shorter wavelength) part of the spectrum compared to red (longer) wavelengths. Also, the signals from the regions with larger primary particle size decay more slowly than the signals associated with smaller particles. The LII model, on the other hand, somewhat overpredicts the conductive cooling rate (see Fig. 6). This essentially means one of two things. Either the conductive cooling equations in the model are incorrect, or the soot particle conditions, e.g., temperature and size, at the end of the vaporization period are incorrectly predicted by the model. The latter would mean the physics during the vaporization-dominated period are incorrectly modeled.

We considered that both particle size and physical changes in the soot through the flame may have an effect on C. As laser fluence may have an influence on both of these, we also consider the possibility that laser fluence might also have an effect on C.

6
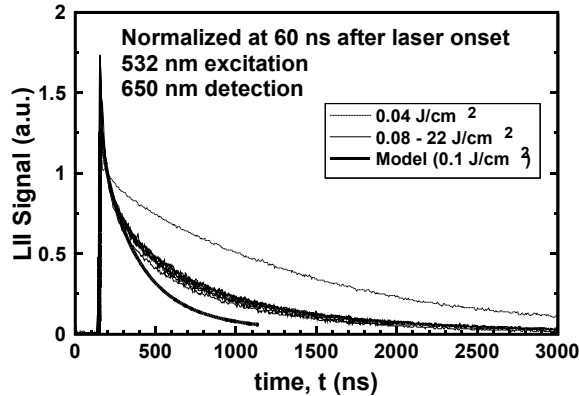
Figure 6. LII time traces for 40 mm HAB (33 nm particle) at various laser fluences. The broken line represents a case below the threshold intensity, while the solid curves range from threshold to over 200 times that fluence. The bold line represents a numerical simulation of the experiment at threshold (0.1 J/cm^2).

Figure 6 shows the the LII signals generated with various laser intensities and reveals the signal decay rate to be independent of laser intensity beyond the threshold fluence. The model, on the other hand, predicts an increase in the decay rate for higher intensities. The model suggests that higher laser intensities result in a hotter but smaller particle (due to vaporization mass loss) at the end of the laser pulse. Therefore, the discrepancy with the experimental data is even greater for higher modeled laser fluences. The similarity of the signal decay above the threshold fluence suggests that the model overpredicts the vaporization effect.

We also attempted to measure particle sizes in the flame by the pyrometric (maximum temperature) technique. Ratios of signals at 650 nm and 430 nm wavelengths were detected for different soot primary particle sizes. Again, these signals are measured at different heights in the flame at the radial maximum soot concentration, and at the side of the flame nearest the detector. Unfortunately, these experiments yielded signal ratios which were either flat or slightly increasing with primary particle size, depending on experimental conditions and laser fluence. The model, recall, predicts a decrease in the spectral signal ratio with increasing primary particle diameter.

It is worth noting one influential effect, that changing the measurement position in the flame yields a change in the signal ratio. Measurements performed at the side of the flame nearest the laser exhibited spectral ratios that increased ~40% more across the particle size range than at the side nearest the detector. The difference in these signal ratio trends is likely due to

different levels of signal trapping on the two channels by soot between the detection volume and the detector. The unexpected behavior of the spectral signal ratio is not encouraging for making size measurements via the pyrometric technique. The fact that different particle sizes may peak at similar temperatures also raises the question as to whether the same result may apply for varying laser energy. Models predict that above the threshold value, we will increase the maximum temperature and decrease the particle size (by vaporization). Both of these should increase the signal decay rate, however, which is contrary to Fig. 6.

In order to examine this issue, the LII signal was observed at one environmental condition (height in flame, particle size) while the excitation energy was varied. First, spectrally resolved LII signals were obtained for different laser fluences.
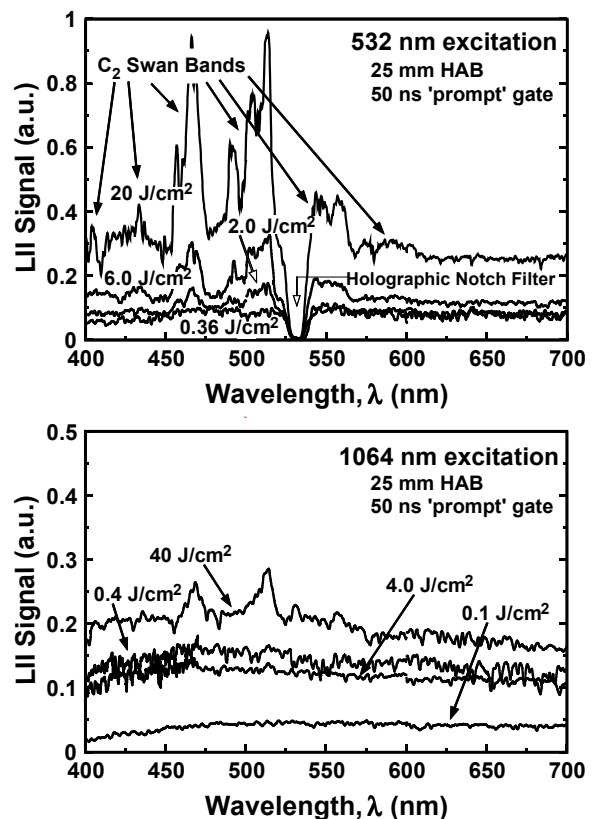
Figure 7. LII spectra recorded in the diffusion flame at a height of 25 mm. Visible wavelength spectra are shown for green and IR excitation and a wide range of excitation energies. The data are corrected for the response of the detection system and spectral emissivity of the soot particles.[25] Arbitrary vertical scales of the two plots are correct relative to one another.

7

The prompt LII emission spectra across the visible wavelengths are displayed in Fig. 7 for both 532 and 1064 nm excitation, and for laser fluences near and above the threshold values. Emission from the C_2 Swan bands is evident at very high laser fluences. Possibly due to a near resonance between the 532 nm excitation and the Swan bands, the C_2 contribution appears much faster for the green excitation than for IR excitation, which has little C_2 interference even at the highest fluences. Also, blackbody curve fits reveal that the spectral shape of the LII signal, and therefore the average soot particle temperature, remain essentially constant for laser intensities above the threshold fluence. An exception to this conclusion is the higher intensity green data, which are hard to fit through the C_2 interference. The curves could be compared at shortly delayed times (e.g., 25 ns), however, and do show the same effect. Spectral ratios of the LII peak signals (~2 ns gate) above threshold yield a constant to within 5%. At 4000 K, this would correspond to $\pm$ 100 K. Again, this contrasts with the model prediction of increasing particle temperatures of 4200 to 5100 K for fluences between 0.4 and 40 J/cm^2. This may mean the model does not correctly represent the dependence of the vaporization rate on temperature.

As the peak temperatures (signal ratios) and signal decay rates level out at the threshold energy, so then should the overall LII signal. Indeed, for a range of energies above the threshold value, the integrated LII signal remains relatively constant (more so, for green excitation than IR). This effect is illustrated in the plots of Fig. 8. LII signals integrated over 50 ns are plotted against laser fluence for both IR and green excitation using prompt detection and, in one case, detection delayed 80 ns from the signal onset. If a situation (e.g. a long absorbing laser path length) motivates the need for energies far above the 'threshold' value, a constant LII response function should be achievable for at least a dynamic range of 10 in laser fluence. The reason why the 'plateau' region is flatter for the green data than for the IR data is unknown. It could be an effect, though, of differing beam focal widths, as the control volume being observed is a very narrow, curved region and the detector is looking tangentially to this. The soot in the imaged volume for the IR case may see a more uniform beam than the other

Beyond the LII threshold fluence for both excitation sources, where vaporization should be reducing the LII signal, another mechanism is driving the signal back up. One can see this high energy contribution is both broadband (see spectral plots) and relatively long-

lived (see 80 ns delay data). At least some of this signal can be attributed to C_2 emission. Considering the 516 nm Swan line with 532 nm illumination, where the C_2 contribution dominates, this interference seems to scale linearly with laser fluence. On a non-logarithmic plot, it is more apparent that the other data is scaling linearly in this region as well.
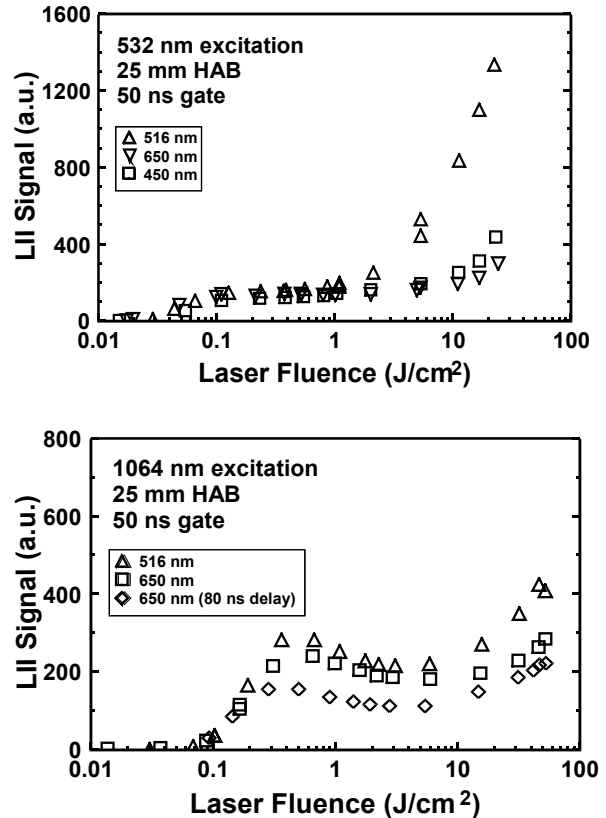
Figure 8. Prompt 50 ns integrated LII signals in the diffusion flame versus incident laser fluence. Signals are recorded at 650 nm, 430 nm and the $\Delta v = 0$ Swan band head at 516 nm. Arbitrary vertical scales of the two plots are correct relative to one another.

While the unknown signal appears to be broadband and long-lived, a non-LII (non-blackbody) type of signal may be indicated. The magnitude of the signal increase after the 'plateau' region is rather large. Fitting blackbody curves to the spectral data above, one finds this increase would involve a significant change in spectral shape for a blackbody, which is not evidenced. However, excitation at these sort of intensities is not likely to be necessary for measuring either concentration or particle size.

In summary, the results above indicate that, above the threshold fluence, not only are different sized parti-

cles attaining the same temperature (recall pyrometric results), but that increasing laser fluence also does not affect this value. It could be that the particles attain some saturation level of energy density and cease absorbing further laser light. At least on an average basis through the profile of the beam, there appears to be little vaporization in the 'plateau' region as both the signal magnitude and shape are insensitive to increasing laser fluence. Another indicator is the fact that the C_2 interference with green excitation does not begin until the end of this region. If the green laser couples to the Swan bands well, there is apparently little C_2 present before this point. However, the significant fraction of vaporization may occur through other species like C_3. Also, other research[10] has suggested that significant vaporization occurs well before this point. Transmission electron microscopy (TEM) images suggest severe mass loss. Even if the vaporization was occurring from the inside out (particle size remaining constant), the decay rate should still increase due the lower mass. If significant vaporization does occur, then some other mechanism must counter the effect this should have on the signal. It is possible that the growth of signals in the wings of the Gaussian beam continuously makes up for the vaporized soot to yield exactly the same spatially-integrated signal for the entire range of signals. One might consider also that the conductive cooling rate is hampered by a cloud of hot gases which comes from and surrounds the particles.

While the discrepancy between the LII and extinction concentration measurements seems to be too large (and monotonic) to be the result of a varying local gas temperature or particle size, we have not ruled out differences in soot composition or morphology (shape or agglomeration). These changes could occur as the soot particle traverses the flame or could occur during the laser-induced heating. There is significant evidence in other research[10,26], that structural and optical properties of soot are changed by laser pulse heating. It is not unreasonable to expect that such changes may also happen thermally through the life of the soot particle as it traverses the flame.

Other possible sources of error that have been ruled out include scattering, and fluorescence, e.g., PAH and C_2 fluorescence. The optical filters have been shown to provide sufficient scattering rejection, and the possibility of fluorescence interference has been investigated using delayed gating/detection. The delayed signals exhibit the same dependence on particle size as the prompt (during laser pulse) data.

As an alternate and idealized soot source and an environment representative of an exhaust flow, experiments have also been performed in the soot generator. This environment is designed to be free of the uncertainties engendered by variations in temperature, chemistry, soot composition or morphology, signal trapping, and adsorbed hydrocarbons. This exhaust flow should also be the best alternative for isolating the effects of different laser intensities. Simultaneously, comparing the behavior of the LII signals in these two environments can help determine the robustness of the LII process to differences in soot properties. The soot in this simulated exhaust flow is expected to be similar to aged (dehydrogenated), less branchy (agglomerated) soot from a combustion process, but may actually represent a very different kind of soot from that in the flame.

Soot Generator

In an effort to calibrate the two environments to each other, measurements were made in both soot fields with the detection setup held constant (focused IR beam (0.5 J/cm^2), broadband detection). The comparison revealed the flame to have a C value 3.7 times greater than that of the soot generator data. The model would predict the difference in local gas temperature (400 and 2000 K) to have an effect of perhaps 1.3. The particle size in the soot generator is expected to be somewhat larger (due to detection constraints) than that in the flame, but if the discrepancy were corrected, the difference in C for the two cases should worsen. The remainder of the difference could be symptomatic of soot particles with notably different properties. Also of note is the fact that the red / blue signal ratio was 50% higher for the flame data. This would suggest the particles in the soot generator were reaching significantly higher temperatures (+800 K for 4000 K flame particles) or that the emissivities were markedly different.

To help clarify the above uncertainty, an analysis similar to that performed for the flame was made for comparison. LII signals were recorded at the exit of the soot generator for various laser fluences, both focused and unfocused beams, and varying soot concentrations. Figure 9 displays the signals generated with an unfocused 1064 nm beam, prompt 50 ns detection, and two soot concentrations. The 10 part per trillion (ppt) (0.02 mg/m^3) soot density was chosen to yield a particle size (~35 nm) similar to that of the primary particles present in the diffusion flame. The signals at low fluences seem to line up well with the results from the

9

flame, including the location of the LII threshold. However, at higher energies, it appears as if the signal is beginning to grow again much sooner than occurred with the flame data. The highest energy in the plot using this concentration (~1.3 J/cm^2) was the maximum energy attainable without focusing the laser beam. Focusing the beam to achieve higher fluences required the use of higher soot concentrations to yield a measurable signal, due to the reduced size of the signal-emitting region.
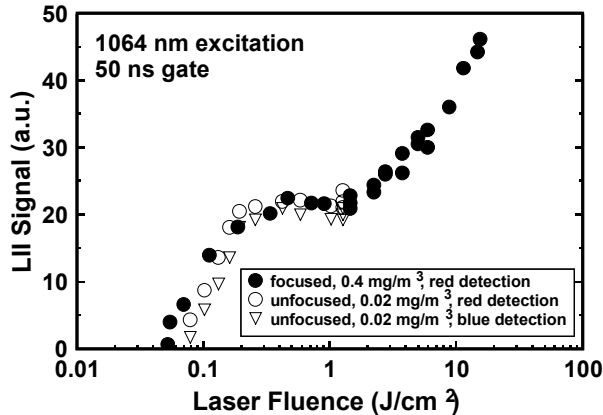
Figure 9. Prompt 50 ns integrated LII signals in the simulated exhaust versus incident laser fluence (IR). Signals are recorded with both the red and blue broadband Schott glass combinations using 0.02 mg/m^3 and an unfocused beam. Also plotted are signals acquired in the red using 0.4 mg/m^3 and a focused beam.

Figure 9 also displays the behavior of the LII signal with laser fluence using a focused beam and approximately 100 nm particles (0.4 mg/m^3). This data agrees well with the lower concentration data and completes the trend. Indeed, the signal does seem to rise above the 'plateau' level at a lower fluence than in the flame data. Again, whatever the mechanism for this might be, this sort of fluence level will likely never be required in typical LII measurements. Also, the agreement of the two data sets shows there is no significant (e.g., beam shape) effect engendered by switching from an unfocused to a focused laser. However, the difference in the flatness of the flame and soot generator curve using a focused IR beam may represent the difference in having a uniform or non-uniform soot field.

Higher soot loading must also be used when employing the monochromator for spectral information, due to the reduced image width and spectral bandwidth. Figure 10 reveals the spectral signature of the LII signal using a full-power, unfocused, 532 nm beam (0.7 J/cm^2) and also the spectra generated with very

high fluence (12 J/cm^2), for both green and IR excitation, at 17 mg/m^3.
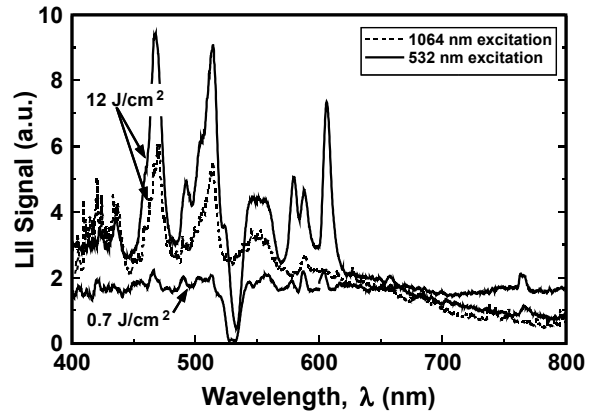
Figure 10. LII spectra recorded in the simulated exhaust flow. Visible wavelength spectra are shown for green excitation at high energy (12 J/cm^2) and IR excitation at the same high energy and at a 'plateau' value of 0.7 J/cm^2. The data are corrected for the response of the detection system and spectral emissivity of the soot particles.[25] Scale of the two high fluence curves are correct relative to one another, while the lower fluence curve is simply scaled for presentation purposes.

A few differences from the flame spectra are quickly noted. A few large spikes are present near 600 nm and a smaller one at 760 nm which are not seen in the flame data. These structures are very likely the emissions of O_2 and O_2^+, representing the beginning of laser-induced breakdown of the surrounding gases which was not apparent by eye or ear. This difference is not surprising considering that the flame soot should be in a rather oxygen-starved environment until high in the flame.
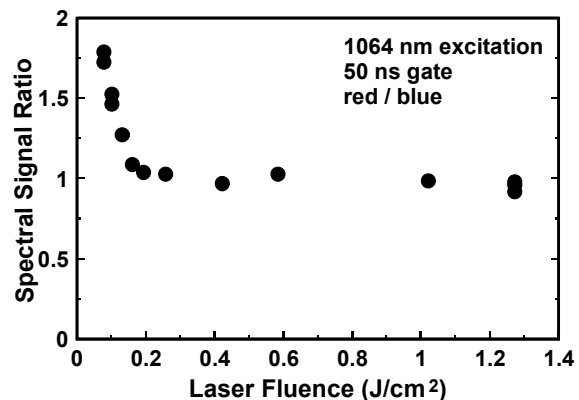
Figure 11. Ratio of red to blue signals recorded in Fig. 9 with the unfocused IR beam.

10

American Institute of Aeronautics and Astronautics

Also, once again the temperatures (the spectral ratios) across the 'plateau' region are constant to within 5%. The ratios of red to blue signals generated in the 0.02 mg/m^3 flow with an unfocused beam are shown in Fig. 11. Signal decay rates are also constant across this region.

Conclusions

LII measurements were performed in two very different environments, a well-documented flame and a simulated engine exhaust. In the flame, some problems have been encountered in attempting to compare the signal from the laser-induced incandescence of soot with the local soot volume fraction measured by laser extinction. Model results and previous measurements in the soot generator suggest that the variation in primary particle size is a candidate for this effect as larger particles should reach higher temperatures and therefore emit more signal per volume of soot. Attempting to utilize this prediction, an attempt was made to measure primary particle size pyrometrically, recording the various peak temperatures via a ratio of long and short wavelength signals. Particle sizing was not successful with this technique as it revealed that the particles of varying sizes are reaching essentially identical peak temperatures, $\pm$ 100 K within the measurement error.

The signal decay rate method of particle sizing did prove sensitive to particle size, however. A numerical simulation of the experiment was performed in hopes of getting a grasp on the physics of the process and to provide a simple calibration for this sizing technique. The model overpredicted the cooling rate noticeably. This could be due to an error in the heat conduction equation, but it seems more likely that the particle properties at the end of the vaporization-dominated period are mistaken. The spectral ratio results show that the model overpredicts the particle superheating.

The spectral ratio was also found to be independent of laser fluence above the threshold fluence, indicating particle temperatures are constant for a very large range of excitation energy. Interestingly, the signal decay rate also does not vary above threshold. Considering these two factors, it is not surprising that the integrated LII signal can be nearly constant past the threshold level. This would appear to be somewhat sensitive to beam shape effects. At higher fluences, the LII signal increases linearly due to some unknown factor and some influence of C_2 emission, depending on excitation and detection wavelength.

The insensitivity of the decay rates with laser fluence suggests that either little or no vaporization is occurring (contrary to the TEM results of other research) or that some other mechanism is countering the effect of vaporization, for instance the effect of a growing cloud of vaporization products on the conductive cooling rate.

The pyrometric results also indicate that particle size is not the basis for the errors encountered in the soot concentration data. In support of this is the fact that primary particle sizes fall to each side of 40 mm HAB, while the measured error behaves monotonically. Local gas temperature should also not be an issue at 'prompt' times. Therefore, an effect by some change in soot property through the flame is indicated. This could involve a variation in shape or agglomeration or a physical property of the soot.

Despite the many differences in the flame and simulated exhaust environments, distinct similarities exist between the two in terms of response to laser fluence. However, evidence for the effect on LII of a change in soot property may exist in the difference in C for the two environments. This relative difference is near 3 after accounting for gas temperature. The carbon black used in the soot generator is also soot, but is aged and may very well have a different internal structure or composition.

Acknowledgments

References

[1]Wilson, R. and Spengler, J. (Ed.), *Particles in Our Air*, Harvard University Press, 1996 p.41-62.

[2]Klingenberg, H., *Automobile Exhaust Emission Testing: Measurement of Regulated and Unregulated Exhaust Gas Components, Exhaust Emission Tests*, Springer Series in Environmental Engineering, Springer-Verlag, New York, 1996, p.103-119.

[3]Dobbins, R. A., Fletcher, R. A., and Lu, W., "Laser Microprobe Analysis of Soot Precursor Particles and Carbonaceous Soot", *Combust. and Flame*, 100, 301-309, (1995).

American Institute of Aeronautics and Astronautics

[4]Köylü, Ü. Ö., McEnally, C. S., Rosner, D.E., and Pfefferle, L. D., "Simultaneous Measurements of Soot Volume Fraction and Particle Size / Microstructurein Flames Using a Thermophoretic Sampling Technique," *Combust. Flame* 110: 494-507 (1997).

[5]Puri, R., Richardson, T. F., Santoro, R. J., and Dobbins, R. A., "Aerosol Dynamic Processes of Soot Aggregates in a Laminar Ethene Diffusion Flame," *Combustion and Flame*, 92, 320-333, (1993).

[6]Santoro, R.J., Yeh, T. T., Horvath, J. J., and Semerjian, H. G., "The Transport and Growth of Soot Particles in Laminar Diffusion Flames," *Combustion Science and Technology,* 53, 89-115, (1987).

[7]Bockhorn, H. (Ed.), <u>Soot Formation in Combustion (Mechanisms and Models)</u>, Springer Series in Chemical Physics 59, Springer-Verlag, New York, (1994).

[8]Eckbreth, A. C., "Effects of Laser-Modulated Particle Incandescence on Raman Scattering Diagnostics," *J. Appl. Phys.,* 48, 4473-4479, (1977).

[9]Ni, T., Pinson, J. A., Gupta, S., and Santoro, R. J., "Two-Dimensional Imagingof Soot Volume Fraction by the Use of Laser-Induced Incandescence," *Applied Optics,* 34, No. 30, 7083-7091, (1994).

[10]Vander Wal, R. L., Ticich, T. M., and Stephens, A. B., "Optical and Microscopy Investigations of Soot Structure Alterations by Laser-Induced Incandescence," *Applied Physics B,* 67, No. 1, 115-123, (1998).

[11]Will, S., Schraml, S., and Leipertz, A., "Comprehensive Two-Dimensional Soot Diagnostics Based on Laser-Induced Incandescence (LII)," 26th Symposium (International) on Combustion*,* 2277-2284, (1996).

[12]McManus, K. R., Frank, J. H., Allen, M. G., and Rawlins, W. T., "Characterization of Laser-Heated Soot Particles Using Optical Pyrometry," AIAA Conference Paper 98-0159, 36th AIAA Aerospace Sciences Meeting and Exhibit, Reno, NV, (1997).

[13]Mewes, B., and Seitzman, J. M., "Soot Volume Fraction and Particle Size Measurements with Laser-Induced Incandescence," *Appl. Opt.,* 36, 709-717, (1997).

[14]Bengtsson, P.-E. and Alden, M., "Soot Visualization Strategies Using Laser Techniques," *Applied Physics B,* 60, 51-59, (1995).

[15]Vander Wal, R. L., and Weiland, K. J., "Laser-Induced Incandescence: Development and Characterization Towards a Measurement of Soot-Volume Fraction," *Applied Physics B,* 59, 445-452, (1994).

[16]Shaddix, C., and Smyth, K., "Laser-Induced Incandescence Measurements of Soot Production in Steady and Flickering Methane, Propane, and Ethylene Diffusion Flames," *Combustion and Flame,* 107, 418-452, (1996).

[17]Quay, B., Lee, T. W., Ni, T., and Santoro, R. J., "Spatially Resolved Measurements of Soot Volume Fraction Using Laser-Induced Incandescence," *Combust. and Flame,* 97, 384-392, (1994).

[18]Vander Wal, R. L., Zhou, Z., and Choi, M. Y., "Laser-Induced Incandescence Calibration via Gravimetric Sampling," *Combust. and Flame,* 105, 462-470, (1996).

[19]Vander Wal, R. L. and Dietrich, D. L., "Laser-Induced Incandescence Applied to Droplet Combustion," *Appl. Opt.*, 34, No. 6, 1103-1107, (1995).

[20]Dec, J. E., zur Loye, A. O., and Siebers, D. L., "Soot Distribution in a D.I. Diesel Engine Using 2-D Laser-Induced Incandescence," SAE Paper 910224, (1991).

[21]Pinson, J. A., Mitchell, D. L., Santoro, R. J., Litzinger, T. A., "Quantitative, Planar Soot Measurements in a D.I. Diesel Engine Using Laser-Induced Incandescence and Light Scattering," SAE Paper 932650, (1993).

[22]Case, M. E., and Hofeldt, D. L., "Soot Mass Concentration Measurements in Diesel Engine Exhaust Using Laser-Induced Incandescence," *Aerosol Sci. and Tech.*, 25, 46-60, (1996).

[23]Wainner, R. T., Seitzman, J. M., and Martin, S. R., "Quantitative Limitations of Laser-Induced Incandescence in Practical Combustion Environments," AIAA Conference Paper 98-0398, 36th AIAA Aerospace Science Meeting and Exhibit, Reno, NV, (1998).

[24]Hess, C. F., "Photothermal Laser Deflection, an Innovative Technique to Measure Particles in Exhausts," Air Force Report (Environics Division) ESL-TR-90-16 (1993).

[25]Hofeldt, D. L., "Real-Time Soot Concentration Measurement Technique for Engine Exhaust Streams" SAE Paper 930079, (1993).

[26]Vander Wal, R. L., Choi, M. Y., and Lee, K.-O., "The Effects of Rapid Heating of Soot: Implications When Using Laser-Induced Incandescence for Soot Diagnostics," AIAA Conference Paper 96-0538, 34th AIAA Aerospace Sciences Meeting and Exhibit, Reno, NV, (1996).